



Resistance profiling of *Aspergillus fumigatus* to olorofim indicates absence of intrinsic resistance and unveils the molecular mechanisms of acquired olorofim resistance

Jochem B. Buil^{a,b}, Jason D. Oliver^c, Derek Law^c, Tim Baltussen^a, Jan Zoll^{a,b}, Margriet W. J. Hokken^a, Marlou Tehupeiry-Kooreman^{a,b}, Willem J. G. Melchers^{a,b}, Mike Birch^c and Paul E. Verweij^{a,b}

^aDepartment of Medical Microbiology, Radboud University Medical Center, Nijmegen, Netherlands; ^bRadboudumc-CWZ Center of Expertise for Mycology, Nijmegen, Netherlands; ^cF2G Ltd, Manchester, UK

ABSTRACT

Olorofim (F901318) is a new antifungal currently under clinical development that shows both *in vitro* and *in vivo* activity against a number of filamentous fungi including *Aspergillus fumigatus*. In this study, we screened *A. fumigatus* isolates for intrinsic olorofim-resistant *A. fumigatus* and evaluated the ability of *A. fumigatus* to acquire an olorofim-resistant phenotype. No intrinsic resistance was found in 975 clinical *A. fumigatus* isolates. However, we found that isolates with increased olorofim MICs (> 8 mg/L) could be selected using a high number of conidia and olorofim exposure under laboratory conditions. Assessment of the frequency of acquired olorofim resistance development of *A. fumigatus* was shown to be higher than for voriconazole but lower than for itraconazole. Sequencing the *PyrE* gene of isogenic isolates with olorofim MICs of >8 mg/L identified various amino acid substitutions with a hotspot at locus G119. Olorofim was shown to have reduced affinity to mutated target protein dihydroorotate dehydrogenase (DHODH) and the effect of these mutations was proven by introducing the mutations directly in *A. fumigatus*. We then investigated whether G119 mutations were associated with a fitness cost in *A. fumigatus*. These experiments showed a small but significant reduction in growth rate for strains with a G119V substitution, while strains with a G119C substitution did not exhibit a reduction in growth rate. These *in vitro* findings were confirmed in an *in vivo* pathogenicity model.

ARTICLE HISTORY Received 30 November 2021; Revised 20 January 2022; Accepted 23 January 2022

KEYWORDS Aspergillosis; F901318; virulence; antifungal resistance; fungal

Introduction

It is estimated that around 250,000 people worldwide suffer from invasive aspergillosis annually [1]. Patients at risk include those with neutropenia and in recent years cases have been increasingly observed in intensive care unit patients, including those with severe influenza or coronavirus infection [2–6]. The triazoles voriconazole and isavuconazole are the recommended first line agents for the management of invasive aspergillosis [7,8]. The use of other registered antifungal agents such as liposomal amphotericin B is limited due to toxicity while the echinocandins exhibit lower efficacy against *Aspergillus* compared to the triazoles [9,10]. Furthermore, the triazoles are currently the only agents that can be administered orally. However, the use of triazoles is threatened by the emergence of azole resistance in *Aspergillus fumigatus* [11], which has now been reported globally [12,13]. Voriconazole resistance in *A. fumigatus* infection was associated with a near doubling of mortality at day 42 compared to voriconazole susceptible infection in patients that

were treated with voriconazole [14]. Azole resistance is mainly driven by environmental exposure of *A. fumigatus* to azole fungicides, which selects for fungicide resistance mutations that confer cross resistance to medical triazoles [15]. In regions with environmental resistance, any patient may present with azole-resistant invasive aspergillosis that complicates diagnosis and successful therapy. Thus, there is an urgent need for new antifungal agents with efficacy against both azole-susceptible and azole-resistant *A. fumigatus* infection.

Olorofim (F901318) is a new antifungal currently under clinical development that shows activity against a number of filamentous fungi including *A. fumigatus*. It belongs to a new orotomide class of antifungals and acts by selective inhibition of fungal dihydroorotate dehydrogenase (DHODH), an essential enzyme within the *de novo* pyrimidine biosynthesis pathway [16,17]. The spectrum of activity of olorofim includes *Aspergillus* species including cryptic *Aspergillus* species and azole-resistant *Aspergillus* isolates [18–25], *Lomentospora prolificans*, *Scedosporium* species

CONTACT Jochem B. Buil ✉ jochem.buil@radboudumc.nl

Supplemental data for this article can be accessed at <https://doi.org/10.1080/22221751.2022.2034485>.

© 2022 The Author(s). Published by Informa UK Limited, trading as Taylor & Francis Group, on behalf of Shanghai Shangyixun Cultural Communication Co., Ltd. This is an Open Access article distributed under the terms of the Creative Commons Attribution License (<http://creativecommons.org/licenses/by/4.0/>), which permits unrestricted use, distribution, and reproduction in any medium, provided the original work is properly cited.

[17,26–30], agents of endemic mycoses such as *Coccidioides* species, *Histoplasma* species, *Sporothrix schenckii* and *Blastomyces* species [17,31]. Furthermore, *in vitro* studies show activity against *Madurella mycetomatis* [32], *Microascus/Scopulariopsis*, *Penicillium*, *Paecilomyces*, *Purpureocillium*, *Rasamsonia*, *Talaromyces* species [17,33,34], dermatophytes [34] and some *Fusarium* species [35]. The *in vitro* activity was confirmed in *in vivo* models for pulmonary aspergillosis with azole-susceptible and azole-resistant isolates of *A. fumigatus* [17,25], in a murine model of disseminated *A. terreus* aspergillosis [36], a murine model of chronic granulomatous disease infected with *A. fumigatus*, *A. nidulans*, and *A. tanneri* [21] and in a murine model of central nervous system coccidioidomycosis [31].

Antifungal drug resistance may develop through genetic variation that is created by the fungus to enable its adaptation to stress factors in its environment. Although drug exposure is not relevant to the development of resistance mutations per se, antifungal drug selection pressure is critical to create dominance of resistant cells within a population of fungal cells. The risk of resistance selection to a new class of antifungal drugs such as the orotomides will depend on the frequency of spontaneous mutations that confer an orotomide-resistant phenotype and the extent of selection pressure through patient therapy. In this study, we screened for intrinsic olorofim-resistant *A. fumigatus*, evaluated the ability of *A. fumigatus* to develop an olorofim-resistant phenotype, and characterized underlying olorofim resistance mechanisms, including the effect of mutated DHODH on olorofim affinity and the impact of resistance mutations on virulence in a mouse model of disseminated aspergillosis. Lastly, the effect of mutated DHODH on conferring olorofim resistance in *A. fumigatus* was proven by introducing the mutation in a wildtype *A. fumigatus* strain.

Material and methods

Agar-based screening of resistance

We screened 976 clinical *A. fumigatus* isolates that were cultured between 2015 and 2017 for non-wildtype olorofim phenotypes. Inoculum with a density of approximately 0.5 McFarland was prepared in sterile 0.9% NaCl with 0.1% Tween 20 and one drop of 25 µl was used to inoculate an agar plate (RPMI1640 (Gibco) with 2% glucose (Merck), buffered with MOPS (Sigma)) containing 0.125 mg/L olorofim. An agar plate containing only RPMI1640 with 2% glucose agar was used as growth control. Olorofim MIC-testing was performed on isolates growing on the agar plate containing olorofim. If routine susceptibility results indicated resistance to voriconazole or itraconazole, the *Cyp51A* gene was subsequently sequenced.

Minimal inhibitory concentration of olorofim

Susceptibility testing was performed using the EUCAST method for susceptibility testing of moulds E.Def.9.3.1 (EUCAST.org). Olorofim pure powder was obtained from F2G (Manchester, United Kingdom). Stock solutions of olorofim were prepared in DMSO (Boom BV). 96-wells plates with 2-fold dilutions of olorofim were prepared in RPMI1640 with 2% glucose and buffered with MOPS. The olorofim concentration range used was 0.016–8 mg/liter. Inoculum was prepared in sterile 0.9% NaCl with 0.1% Tween 20. Spores were harvested from mature culture and the suspension was adjusted to 80–82% transmission at 530 nm (Spectrofotometer Genesys 20) to create a $1\text{--}4.2 \times 10^6$ CFU/ml spore suspension [37]. Inocula were added to the 96-well plates to create a final concentration of $2\text{--}5 \times 10^5$ CFU/ml in each well. The inoculated plates were incubated for 48 h at 35°C. MIC was defined as the lowest concentration without visible growth.

Selection of resistant mutants

Six *A. fumigatus* isolates (ATCC 204305, AZN8196 [38], V052-35 (TR₃₄/L98H) [38], V139-36, V180-37 [39] and V254-51) were used for the olorofim resistance induction experiment. Strains were confirmed to be *A. fumigatus* based on the Beta-tubulin sequence. Sabouraud dextrose broth containing chloramphenicol (SAB-c) was inoculated and cultures were grown at 28°C. Spores were harvested in sterile saline with 0.1% tween 20 and the inoculum was transferred to a sterile vial. The spore suspension was adjusted to 1×10^9 spores/mL using an hemocytometer. One mL spore suspension was added to a 90 mm agar plate containing RPMI 1640 + 2% glucose (1.5% agar) containing 0.5 mg/L olorofim. Cultures were grown at 28°C. Isolates that grew on the olorofim containing plates were subcultured on SAB-c for subsequent MIC testing and DNA isolation.

Frequency of resistance analysis

Six *A. fumigatus* isolates (ATCC 204305, AZN8196, V052-35 (TR₃₄/L98H), V139-36, V180-37 and V254-51) were used for the olorofim resistance induction experiment (Table 2). SAB-c was inoculated using a single spore isolated from the six parent strains and cultures were grown at 28°C. Spores were harvested in sterile saline with 0.1% tween 20 and the inoculum was transported to a sterile vial. The spore suspension was adjusted to 1×10^9 spores/mL using an hemocytometer. One mL spore suspension was added to a 90 mm agar plate containing RPMI 1640 + 2% glucose (1.5% agar) containing either 0.5 mg/L olorofim, 4 mg/L voriconazole (Sigma) or itraconazole (Sigma)

8 mg/L. These concentrations were chosen as these were the concentrations which are 2 dilutions higher than the concentration that inhibits 100% of wildtype *A. fumigatus* isolates [40]. Cultures were grown at 28°C. Isolates that grew on the olorofim containing plates were subcultured on SAB-c for subsequent MIC testing and DNA isolation. The resistance rate was calculated by dividing the number of retrieved resistant colonies by the number of inoculated spores and the mean of 5 experiments was used for comparison. Differences in resistance frequency between olorofim and itraconazole or voriconazole were tested for significance using the student *T*-test. Statistical significance was defined as a *P*-value of ≤ 0.05 (two-tailed). To confirm the resistant rates, a second experiment was performed in another laboratory. Spore stocks of *A. fumigatus* strain Af293 were prepared and inoculated onto yeast nitrogen base with glucose agar (YNBG) containing 0.25 mg/L olorofim. A total of 8×10^9 spores were inoculated into 12×100 ml YNBG agar plates containing 0.25 mg/L olorofim that were subsequently incubated for 5 days at 35°C. Colonies growing on drug-containing plates were subcultured again on YNBG-containing 0.25 mg/L olorofim to confirm resistance.

Sequencing of *PyrE* identifies hotspot at *Gly119*

The *PyrE* gene of all isolates from parent strain Af293 were sequenced as previously described using primers AFDseq-F2 and AFDseq-R2 [18]. *PyrE* amino acid sequences of olorofim-resistant strains were compared to the amino acid sequence of the wildtype parent strains. As these and the earlier pilot experiments showed only amino acid substitutions at locus *G119* without mutations at other loci in *PyrE*, we sequenced only part of the *PyrE* gene for the other strains. This part of the *A. fumigatus* *PyrE* gene was sequenced using primer *PyrE_G119_Fwd*: AGTAAAGGAGG-CACCCAAGAAAGCTGG and *PyrE_G119_Rev*: GCCAATGGGGTTGTTGAGCGTATACCC. We randomly selected 39 olorofim-resistant strains from the resistant frequency analysis.

Olorofim inhibition assays of mutant recombinant DHODH

The cloning of *A. fumigatus* DHODH₍₈₉₋₅₃₁₎ cDNA into protein expression vector pET44 yielding pET44AFD was described previously [17]. For the preparation of mutated protein, this plasmid was mutated at codon 119 using the Phusion Site-Directed Mutagenesis kit (Thermo Scientific). PCR reactions were set up with Phusion HSII polymerase, pET44AFD as a template, with one constant primer (AFDSDM_R1; CCTCTCCGCGTCGGGATAA) and a variable that had a single codon change

(CGCATCATATTxyzGTGGAAGCTCT). The sequence of xyz (GGT in wild type) was: GTT for G119V; GCT for G119A; AGT for G119S; TGT for G119C. The PCR product representing a linear version of pET44AFD with the mutation present was ligated using T4 DNA ligase and transformed into Max Efficiency DH5 α competent cells (Thermo Fisher). Sequencing confirmed the desired mutations were present. The constructs were transformed into *E. coli* BL21 (DE3) cells (Merck) and the mutant proteins were expressed and purified according to the protocol described by Oliver et al [17]. DHODH assays were set up in the presence and absence of olorofim at concentrations between 0.008–100 μ M. Assays were carried out in 50 mM Tris HCl pH8, 150 mM KCl, 10% (wt/vol) glycerol, and 0.1% (wt/vol) Triton X-100 in the presence of 1 mM L-dihydroorotic acid, 0.05 mM coenzyme Q2 and 0.1 mM 2,6-dichloroindophenol as a redox indicator. The reaction was followed by absorbance at 600 nm and reaction velocities used to construct IC50 curves [17]. Curves were fitted in GraphPad Prism using variable slope (four parameters) on log transformed data.

G119 transformations using CRISPR-Cas9

To prove that G119 mutations are resulting in increased olorofim MICs we introduced the G119C mutation in strain MFIG001 [41] as previously described [42]. In short, protoplasts were generated by inoculation of approximately 1×10^6 fresh conidia in Yeast extract Glucose medium (YG; 0.5% yeast extract, 2% glucose) for 16 h at 37°C shaking at 120 rpm. Mycelia were harvested by filtration and resuspended in YG with protoplasting buffer (5 g Vinotaste in 50 mL 1M KCl and 0.1 M Citric Acid added to 50 mL YG) and reincubated for 4 h at 37°C shaking at 100 rpm. Then protoplast was washed 3 times in 0.6 M KCl and 50 mM CaCl₂ and the protoplast concentration was adjusted and diluted to approximately 1×10^6 protoplasts. A PAM site close to the G119 locus was selected with an adjacent 20 nucleotide protospacer that covers the G119 locus using a web-based guide RNA designing tool EuPaGDT [43]. The genome sequence of *A. fumigatus* A1163 (*Aspergillus_fumigatus* A1163.ASM15014v1) was manually uploaded to EuPaGDT to design gRNAs to the *pyrE* locus. The program was carried out with the default settings and the crRNA with the highest QC score closest to the target integration was selected for transformation. A single stranded (ss) DNA repair template was selected that covered 50 nucleotides on both sites of the protospacer and PAM site (Figure s1) that contains a synonymous point mutation in the PAM site and the T > G mutation in the G119 locus resulting in GGT (Glycine) to TGT (Cysteine) transformation.

Alt-R® CRISPR-Cas9 tracrRNA, Alt-R® CRISPR-Cas9 crRNA, Alt-R® S.p. Cas9 Nuclease and ssDNA repair template were ordered from Integrated DNA Technologies. Ribonucleoprotein (RNP) complex was assembled *in vitro* in Nuclease-Free IDTE buffer. RNP complex, the ssDNA repair template and PEG buffer (60% wt/vol PEG3350, 50 mM CaCl₂, 450 mM Tris-HCl, pH 7.5) were mixed with 50 µl of the 1 × 10⁶ /ml protoplast and incubated on ice for 50 min. Then 1 mL of PEG 3350 was added to the solution and incubated for another 25 min at 20°C. The solution was incubated on five yeast extract peptone dextrose (YPD) agar plates and incubated for 48 h. Single colonies were subcultured on SDA slants and screened for resistance by spotting 2 µL containing 100–500 conidia on RPMI1640 2% glucose agar containing 0.125 mg/L olorofim and RPMI1640 2% glucose agar without olorofim as growth control. Five isolates showing prominent growth after 48 h were selected and further analyzed by olorofim MIC testing and sequencing of the *pyrE* G119 hotspot as described earlier.

Radial growth rate

To study the radial growth rate, we randomly selected five olorofim-resistant isolates, two from strain AZN8196 (AZN8196_OLR1, AZN8196_OLR2) and three from strain Af293 (Af293_OLR5, Af293_OLR7, and Af293_OLR9) from the initial induction experiments and compared the radial growth rate to the wildtype parent strain. The strains were chosen as these strains harboured the most common amino acid substitutions G119C, G119V and G119S. We assessed the growth by measuring the colony diameters in the horizontal axis and vertical axis once every 24 h for a period of 5 days. We used an initial inoculum of 2 × 10² spores, quantified with a hemocytometer for all strains and inoculated the spores in the middle of a 90 mm petri dish with Yeast Nitrogen Base with glucose. We did three independent experiments per strain and reported the mean of the three experiments. Differences in growth rate in mm/day at day 5 between wildtype and olorofim-resistant strains were tested for significance using the student *T*-test. Statistical significance was defined as a *P*-value of ≤0.05 (two-tailed).

Assessment of the pathogenicity of olorofim-resistant progeny compared to strain AZN8196 and Af293

To study the virulence of isolates with *PyrE* amino-acid substitution, we assessed the survival of these isolates in a murine model of disseminated aspergillosis and compared the survival to their wildtype parent strains. Ideally, truly isogenic isolates are used for

such experiments. However, the selected isolates were selected for olorofim resistance on a plate and only the *PyrE* gene was sequenced and we thus cannot exclude amino acid substitutions elsewhere in the genome. To exclude effects of such additional substitutions we used five separately selected olorofim-resistant strains to perform the experiments. CD-1 mice (Charles River Laboratories, Margate, UK) were immunosuppressed 3 days prior to infection with cyclophosphamide administered at 200 mg/kg subcutaneously. Inoculum was prepared for *A. fumigatus* strains AZN8196, AZN8196_OLR1, AZN8196_OLR2, Af293, Af293_OLR5, Af293_OLR7, and Af293_OLR9. Mice were infected by intravenous administration of 0.2 mL conidial suspension. An inoculum of approximately 5 × 10⁵ CFU/mL was used for strains AZN8196, AZN8196_OLR1, AZN8196_OLR2 and an inoculum of approximately 2.5 × 10⁷ CFU/mL was used for strains Af293, Af293_OLR5, Af293_OLR7, and Af293_OLR9 resulting in 1 × 10⁵ CFU/mouse and 5 × 10⁶ CFU/mouse respectively. These inocula were chosen as those are the LD₉₀ doses that were previously determined for these specific *A. fumigatus* strains [44,45]. The concentration of conidia was adjusted using a hemocytometer and confirmed by quantitative culture on SDA. Actual and intended inoculum levels are listed in table S2. Eight mice were inoculated with all strains. Mice were monitored for survival for 10 days and euthanized when they demonstrated high weight loss, signs of sepsis or severe torticollis. Survival data were analyzed using GraphPad Prism (Version 5.3) and checked for significance using the Log-rank (Mantel–Cox) Test. Statistical significance was defined as a *P*-value of ≤0.05 (two-tailed).

Results

Agar-based screening of resistance

A total of 976 clinical *A. fumigatus* isolates were screened for olorofim non-wildtypes on agar plates containing 0.125 mg/L olorofim. Only one isolate showed growth on the agar well supplemented with 0.125 mg/L olorofim (isolate V179-44). No growth on plates containing 0.125 mg/L olorofim was seen in the other 975 isolates.

Identification of acquired resistance in *A. fumigatus*

Clinical *A. fumigatus* isolate (V179-44) was identified as possibly olorofim resistant and *in vitro* susceptibility testing using a spore suspension derived directly from the agar well supplemented with 0.125 mg/L of olorofim, showed an olorofim MIC of >8 mg/L. Susceptibility testing from the initial culture of strain

V179-44 resulted in a wildtype olorofim MIC of 0.031 mg/L. Identification of the resistant isolate through beta-tubulin sequencing confirmed the conventional identification as *A. fumigatus* sensu strictu [46]. As we suspected selection of a colony with a spontaneous olorofim resistance mutation, we tried to replicate this observation. Inoculation of $>1 \times 10^9$ spores of three *A. fumigatus* isolates (AZN8196, V052-35 and V139-36) on three 90 mm petri dishes with RPMI1620 agar supplemented with 2% glucose containing 0.5 mg/L olorofim, two olorofim-resistant *A. fumigatus* colonies were retrieved from parental strain AZN8196 (AZN8196_OLR1 and AZN8196_OLR2), three from V052-35 (V052-35_OLR1 to V052-OLR3) and 11 from V139-36 (V139-36_OLR1 to V139-36-OLR11).

In vitro frequency of spontaneous mutations resulting in olorofim resistance in asexual sporulation

Six *A. fumigatus* isolates (ATCC 204305, AZN8196, V052-35 (TR₃₄/L98H), V139-36, V180-37 and V254-51) (Table 1) were used for the resistance frequency experiment. A total of 131 olorofim non-wildtype strains were retrieved, all of which showed an olorofim MIC of >8 mg/L (Table S1). An olorofim resistance frequency of 1.3×10^{-7} – 6.9×10^{-9} was observed (Figure 1). The mean itraconazole resistance frequency was between 1.2×10^{-6} and 3.3×10^{-8} and the mean voriconazole resistance frequency was between 1.8×10^{-8} and 2.0×10^{-10} . Overall, the frequency of resistance was higher for itraconazole compared to olorofim, while voriconazole had the lowest frequency of resistance. The frequency of resistance of olorofim was significantly lower than itraconazole for strains AZN8196 and V254-51, while the frequency was not significantly lower for strains ATCC204305, V139-36 and V180-37. The frequency of voriconazole resistance was significantly lower compared with olorofim for strains ATCC204305, AZN8196, V139-36 and V254-51, while no significant differences were observed for strain V180-37. The second independent resistance frequency analysis using isolate Af293, which was cultured on yeast nitrogen base agar with glucose supplemented with 0.25 mg/L olorofim resulted in a mean frequency of olorofim resistance of 1.7×10^{-9} , a rate comparable

to the above experiments. A total of 11 isolates were retrieved from parent strain Af293 of which 10 had an olorofim MIC of >8 mg/L while one had a MIC of 0.25 mg/L (Table S1).

Sequencing of *pyrE* identifies a hotspot for olorofim resistance at Gly119

The target of olorofim has been identified as the pyrimidine biosynthetic enzyme DHODH, which in *A. fumigatus* is encoded by the *pyrE* gene. When sequencing the full *pyrE* gene of olorofim strains retrieved from parent strain Af293, we found mutations at locus G119 in 10 of 11 sequenced olorofim-resistant isolates. A single isolate with an olorofim MIC of 0.25 mg/L had a *pyrE* sequence identical to the parent Af293 strain. Subsequent analysis of a subset of 39 isolates from the resistance frequency analysis, showed that mutations that resulted in an amino acid substitution at G119 were present in 38/39 isolates. In total 7 isolates had a G119A amino acid substitution, while we found G119C (21 isolates), G119F (1 isolate), G119Y (1 isolates), G119S (11 isolates), and G119V (7 isolates) amino acid substitutions in the other isolates. One olorofim-resistant isolate harboured a H116P amino acid substitution in the *PyrE* gene (Table 2).

Confirmation of the resistance mechanism

We investigated the effect that selected mutations at G119 had on the ability of olorofim to inhibit recombinant *A. fumigatus* DHODH. Recombinant DHODH with the amino acid substitutions G119A, G119V, G119S and G119C showed significantly higher IC₅₀ values for olorofim compared to wildtype DHODH (Figure 2). The substitutions at G119 thus resulted in decreased inhibition of *A. fumigatus* DHODH by olorofim, confirming the olorofim resistance mechanism.

G119 transformations using CRISPR/Cas9

To further prove that the *PyrE* G119 mutations in *A. fumigatus* result in increased MICs to olorofim, we introduced the G119C mutation in *A. fumigatus* by a marker free CRISPR-Cas9 method in strain MFIG001 [41,42]. MFIG001 is a strain deficient in

Table 1. Strains used in this study for resistance frequency analysis.

Strain	Cyp51A genotype	Source	Olorofim MIC (mg/L)	Voriconazole MIC (mg/L)	Itraconazole MIC (mg/L)
ATCC 204305	wildtype	Reference strain	0.016	0.25	0.125
AZN8196	wildtype	Radboudumc fungal database	0.031	0.25	0.125
V052-35	TR ₃₄ /L98H	Radboudumc fungal database	0.031	8	>16
V139-36	wildtype	Radboudumc fungal database	0.063	0.25	0.25
V180-37	wildtype	Radboudumc fungal database	<0.016	0.5	0.5
V254-51	wildtype	Radboudumc fungal database	0.031	0.25	0.5
AF293	wildtype	Reference strain	0.016	0.5	0.5

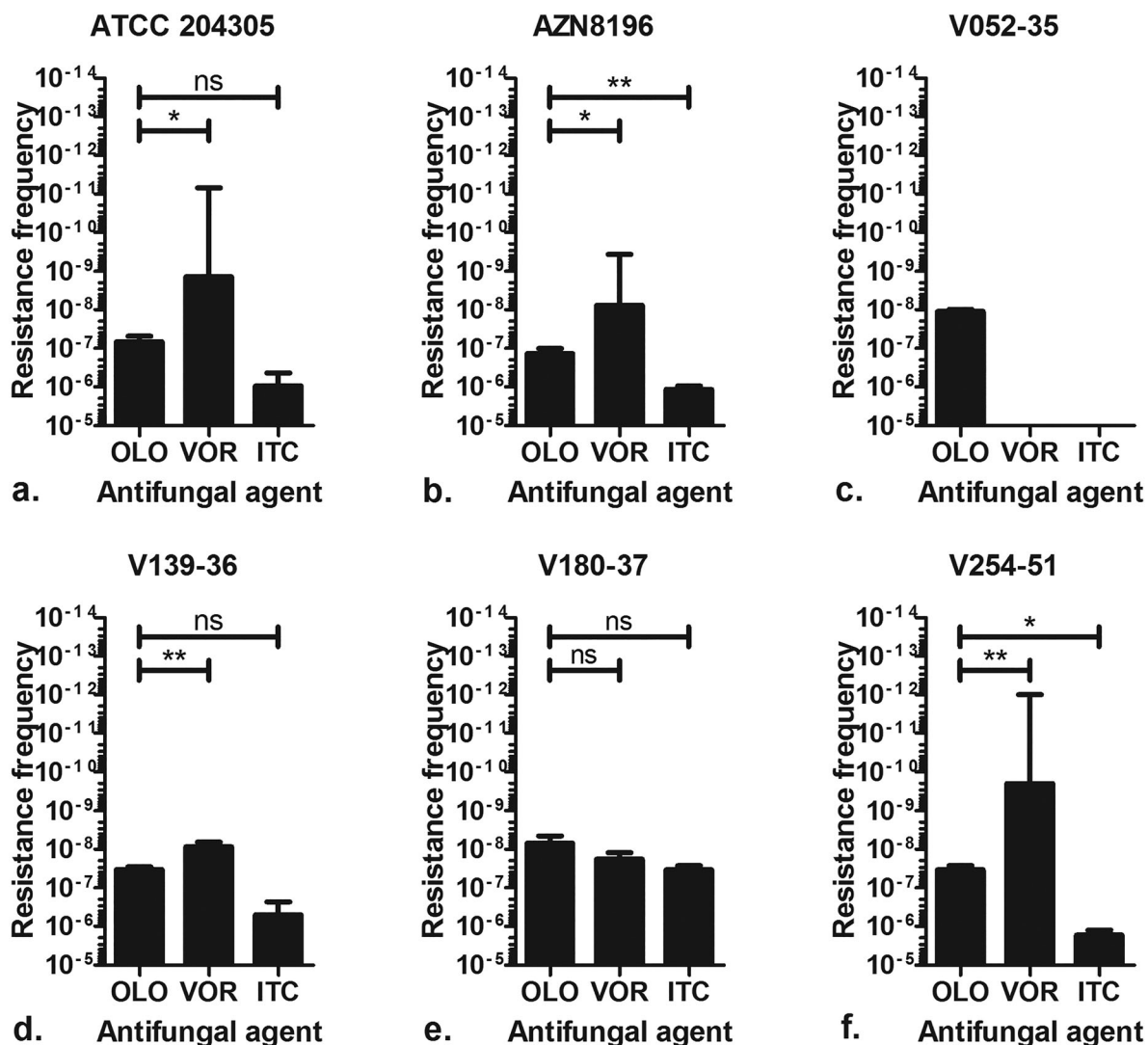


Figure 1. Olorofim resistance frequency. Frequency of resistance observed of six *A. fumigatus* isolates when 10^6 – 10^9 spores were incubated on RPMI agar plates containing either 0.5 mg/L orlofom (OLO), 4 mg/L voriconazole (VOR) or 8 mg/L itraconazole (ITC). *A. fumigatus* ATCC 204305 b. *A. fumigatus* AZN 8196 c. *A. fumigatus* V052-35 (TR₃₄/L98H, azole resistant) d. *A. fumigatus* V139-36 e. *A. fumigatus* V180-37 and f. *A. fumigatus* V254-51. * $P \leq 0.05$ ** $P \leq 0.01$, ns Not significant.

the non-homologous end-joining pathway resulting in a high transformation rate. Single colonies from the transformations were subcultured on Sabouraud dextrose agar (SDA) slants and screened for orlofom resistance on an agar plate containing 0.5 mg/L orlofom. Three strains (MFIG001_pyrE^{G119C}_01, MFIG001_pyrE^{G119C}_03 and MFIG001_pyrE^{G119C}_05) that grew on the orlofom containing plate were selected for *PyrE* sequencing and subsequent MIC testing confirming the presence of G119C mutations

(including the transformation specific synonymous PAM site mutation) (Figure S2) and orlofom MICs of >8 mg/L.

Influence of *PyrE* substitution on radial growth rate

As development of resistance is often associated with attenuated virulence [47], we investigated the effects of orlofom resistance mutations on the fitness of

Table 2. Mutations in the *PyrE* gene in isolates selected for orlofom resistance.

Parent Strain	Cyp51A genotype	Number of orlofom-resistant progeny sequenced strains	<i>PyrE</i> amino acid substitutions					H116P
			G119A	G119C	G119F	G119Y	G119S	
ATCC 204305	wildtype	8	1	5			2	
AZN8196	wildtype	6	2	2			1	1
V052-35	TR ₃₄ /L98H	4		4				
V139-36	wildtype	9	1	4		1	1	2
V180-37	wildtype	4	1	1	1			
V254-51	wildtype	8	2	2			4	
Af293	wildtype	10		3			3	4

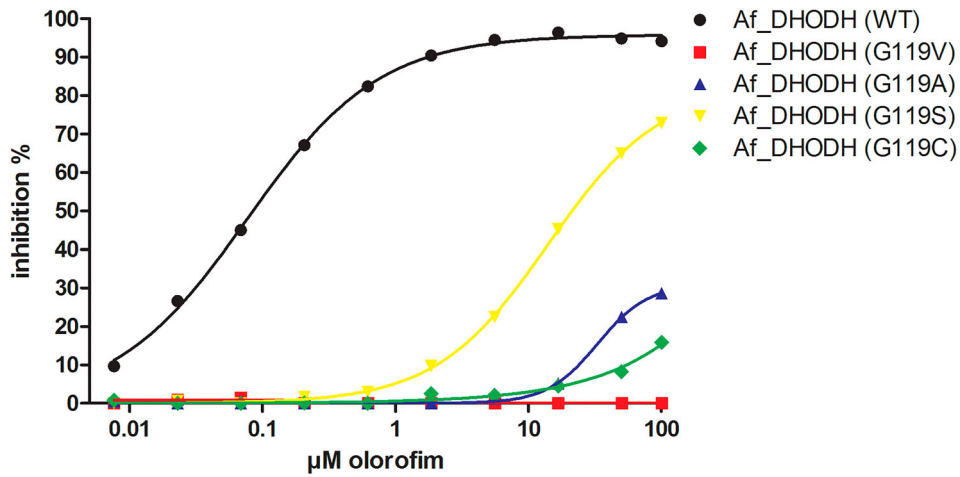


Figure 2. IC50s of wildtype and mutant DHODH. The inhibition of DHODH activity by a range of orlofim concentrations was measured for the recombinant wild type Af293 enzyme and the Gly119 mutants indicated. Lines were fitted using log (inhibitor) vs response – Variable slope (four parameters) in Graphpad Prism. *R* squares were 0.998 for Af_DHODH (WT), 0.556 for Af_DHODH (G119V), 0.924 for Af_DHODH (G119A), 1.000 for Af_DHODH (G119S) and 0.9680 for Af_DHODH (G119C).

A. fumigatus. To assess the impact of the substitution of G119 in the *PyrE* gene on fitness, we used *in vitro* radial growth experiments. Mean growth curves are shown in Figure 3. The mean radial growth at day 5 of AZN8196_OLR1 (carrying the G119V mutation) was 30.7 mm, which was significantly different to the wildtype parent strain AZN8196 which had a mean

growth of 40.0 mm ($p < 0.001$). The mean radial growth of AZN8196_OLR2 (G119C) was 35.8 mm, also slightly reduced compared to strain AZN8196 but not significantly ($p = 0.06$). The mean growth at day 5 was 42.7 mm for Af293, which was not significantly different compared with the mean growth at day 5 of strain Af293_OLR7 (G119C) ($p = 0.349$),

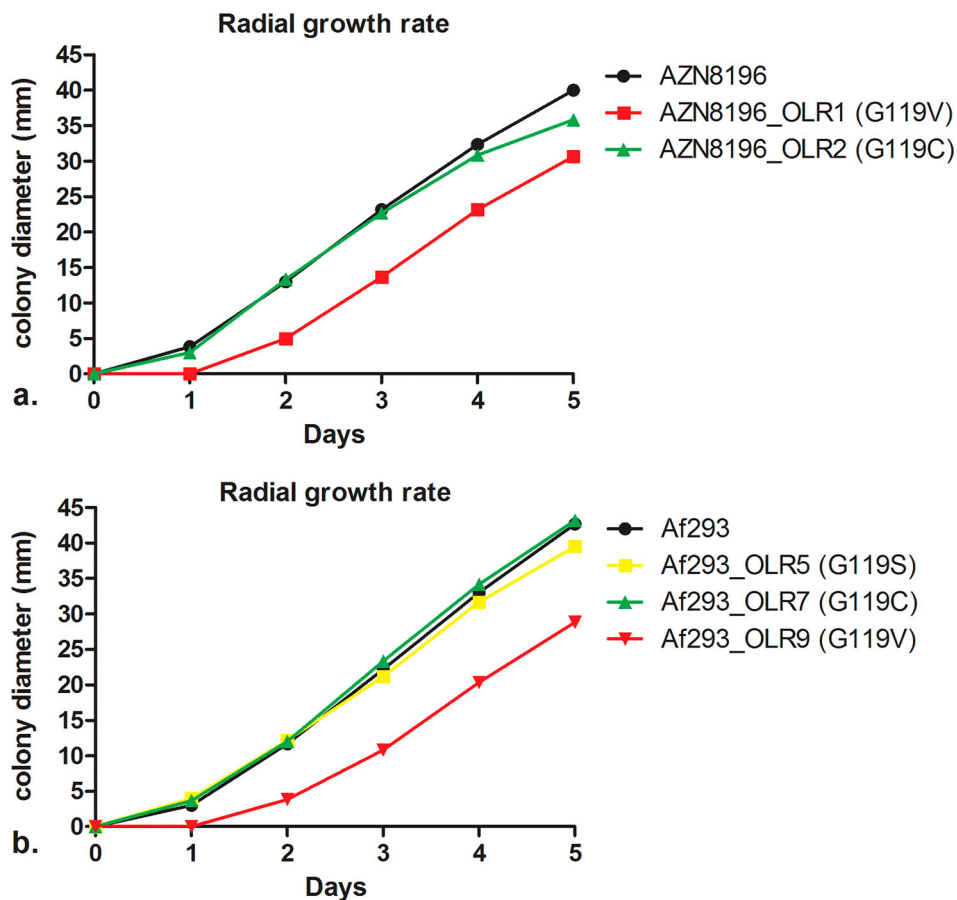


Figure 3. Radial growth rate of isolate AZN8196 and Af293 and orlofim-resistant progeny. Colony diameters are displayed for (a) isolate AZN8196 and 2 orlofim-resistant progeny isolates AZN8196_OLR1 (G119V) and AZN8196_OLR2 (G119C) with and (b) Af293, Af293_OLR5 (G119S), Af293_OLR7 (G119C) Af293_OLR9 (G119V).

which had a mean growth 43.2 mm. The mean 5-day growth of Af293_OLR5 (G119S) was slightly decreased compared to the parent at 39.5 mm ($p = 0.0039$). Once more the glycine to valine mutation had the greater effect on growth with Af293_OLR9 growing 28.8, 14.4 mm less than the parental strain ($p = 0.0010$). Thus, in two different *A. fumigatus* strains the G119V mutants grew significantly more slowly than the parental strain (Figure 3).

Pathogenicity of olorofim-resistant *A. fumigatus* strains in an *in vivo* murine model

Although the radial growth rate experiments did not reveal significant fitness cost for two of the tested isolates, we wanted to confirm these observations in a neutropenic murine infection model. All strains demonstrated virulence with all animals succumbing to disease by 96 h post infection. Median survival times of animals infected with AZN8196, AZN8196_OLR1 (G119V) and AZN8196_OLR2 (G119C) were 68.13, 89.75 and 73.38 h after infection, respectively. Mice infected with AZN8196_OLR1 (G119V) survived significantly longer than those infected with their parent strain. There were no significant differences between mice infected with AZN8196_OLR2 and the parent strain (Figure 4(a)).

Median survival times of animals infected with Af293, Af293_OLR5 (G119S), Af293_OLR7 (G119C), and Af293_OLR9 (G119V) at a concentration of approximately 5×10^6 CFU/mouse were 45.25, 46.75, 48.25 and 55 h post infection, respectively. No difference in survival time was found between animals infected with Af293 and those infected with Af293_OLR5 (G119S) and Af293_OLR7 (G119C). However, Af293_OLR9 (G119V)-infected animals survived significantly longer than Af293-infected mice (Figure 4(b)).

Whilst the other mutants tested appeared as virulent as their parental strains, the two G119V mutant strains generated from different parents survived for longer. This is consistent with the slower growth observed for these strains in the radial growth experiments. These strains appear less fit than the wild type both *in vitro* and *in vivo*.

Discussion

Evaluation of a large collection of clinical *A. fumigatus* isolates showed that the olorofim resistance frequency is negligible and no cross resistance with azoles was detected. However, olorofim resistance can be selected for under laboratory conditions and is associated with point mutations at locus G119 of the *PyrE* gene. Such mutations confer a resistant olorofim phenotype (olorofim MICs >8 mg/L), which appeared to have variable effects on virulence.

Olorofim is a promising novel antifungal with *in vitro* and *in vivo* efficacy against *A. fumigatus* infection, including triazole-resistant cases. The drug is currently undergoing phase II evaluation for the treatment of patients with invasive fungal infections that cannot be managed with current agents. Screening of over 900 clinical *A. fumigatus* isolates showed intrinsic resistance is not identified, confirming the results from susceptibility testing of 1032 clinical *A. fumigatus* isolates from Denmark [18].

Olorofim resistance in *A. fumigatus* has not been reported before. A previous evolution experiment involving 50 passages of *A. fumigatus* exposed to an olorofim concentration gradient, resulted only in a modest olorofim MIC increase. In contrast voriconazole generated a four-fold increase in MIC after only 15 passages [17]. In the present study, we observed the *in vitro* acquisition of olorofim resistance while screening for intrinsic resistance using an agar supplemented with olorofim. All strains that were screened for olorofim resistance using this method were inhibited on this olorofim-containing agar, except one isolate. The olorofim-containing agar well of this strain showed growth of a single colony, in contrast to the growth control that showed confluent growth of numerous colonies on the whole agar surface. Had the initial isolate been resistant, we would have also expected numerous colonies growing in the olorofim-containing agar similar to the growth control. The lack of this growth, together with the discrepant results from the susceptibility testing of the parental colony and the colony growing on the olorofim-containing agar led us to believe that the resistant isolate had acquired olorofim resistance while being cultured on olorofim-containing agar.

By using a high inoculum of 1×10^9 CFU/mL we found that isolates with increased olorofim MICs (>8 mg/L) could indeed be selected confirming our previous observation. As we wanted to understand the implications of this observation, we assessed the frequency of resistance development of *A. fumigatus* to olorofim and compared this frequency to other clinically used triazoles. We have chosen itraconazole and voriconazole as comparator agents as resistance development has been described in patients receiving long-term therapy for (cavitating) chronic pulmonary aspergillosis (CPA) but not in patients treated for acute invasive aspergillosis [48,49]. We found that the resistance frequency of itraconazole was higher than the resistance frequency found for voriconazole. Similar observations are seen in the treatment of patients with CPA where the rate of emergence of azole resistance during therapy was 13% for itraconazole and 5% for voriconazole [50]. Differences in resistance frequency between itraconazole and voriconazole may be explained by the fact that almost all azole resistance associated substitutions reported in

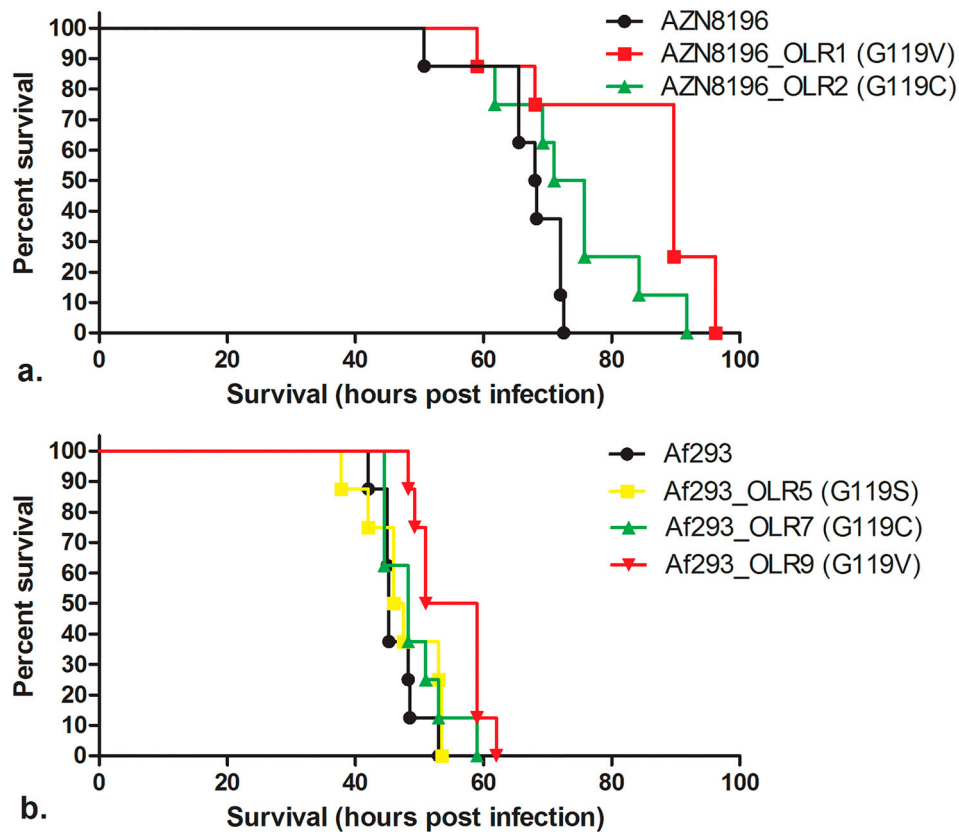


Figure 4. *In vivo* virulence model. Survival of mice inoculated with (a) orlofim wildtype strain AZN8196 and orlofim-resistant progeny AZN8196_OLR1 and AZN8196_OLR2, and (b) orlofim wildtype strain Af293 and orlofim-resistant progeny Af293_OLR5, Af293_OLR7 and Af293_OLR9. Eight mice were inoculated with each strain.

the *Cyp51A* gene result in itraconazole MICs above 4 mg/L, while only few substitutions result in high-level resistance to voriconazole [51]. The finding of spontaneous orlofim resistance mutations is not surprising, but the frequency appears to be relatively low. The conditions that enable *in vivo* selection of orlofim resistance may be similar to those for triazole resistance; a setting of a high number of replicating fungal cells and chronic drug exposure. Such conditions may be present in patients with cavitory pulmonary lesions, such as aspergilloma and CPA but are unlikely in patients with acute invasive aspergillosis. However, as there are currently no alternative anti-fungal agents available for treatment of patients with triazole-resistant CPA that can be administered orally, orlofim represents a promising treatment option for this patient group that requires further clinical evaluation.

Importantly, *in vivo* selection of resistance mutations during treatment is not observed in patients treated for invasive aspergillosis. Triazole resistance in acute invasive aspergillosis is caused by inhalation of triazole-resistant *A. fumigatus* conidia that have developed resistance in the environment through exposure to azole fungicides, which occurred over several decades of exposure [15]. Agents that inhibit DHODH as mode of action are currently not used for crop protection; to prevent a similar scenario to environmental

triazole resistance selection, the use of similar mode of action compounds for medical and environmental applications should be avoided.

DHODH is an essential enzyme in the *de novo* pyrimidine biosynthesis pathway, and disruption of this pathway results in attenuated virulence in *A. fumigatus* [52]. Similar observations are reported in other fungal species like *Candida albicans*, *Cryptococcus neoformans* and *Histoplasma capsulatum* and the necessity of an undisrupted pyrimidine biosynthesis pathway is demonstrated in both *in vitro* and *in vivo* models [53–55]. As DHODH, the product of the *pyrE* gene, is the enzyme target of orlofim action, we hypothesized that the most likely target of resistance is the *pyrE* gene [17]. Indeed, sequencing the *PyrE* gene of isolates with orlofim MICs of >8 mg/L identified various amino acid substitutions. A homology model of the *A. fumigatus* DHODH predicted a potential binding mode for orlofim [17].

Locus G119, located within this binding site was identified as a specific hotspot for orlofim resistance in *A. fumigatus* as 48/49 sequenced isolates had amino acid substitutions at G119. A single isolate had an amino acid substitution at position H116 which was predicted as a key residue for orlofim binding [17]. The effect on orlofim susceptibility of mutations in *PyrE* at locus G119 was proven by both orlofim inhibition assay of mutant recombinant DHODH and by

introducing the *PyrE* G119C mutation directly in *A. fumigatus*.

It remains uncertain whether locus G119 will also be the main mechanism of resistance if olorofim-resistant *pyrE* isolates eventually emerge in clinical practice. Preliminary data shows that several translation factors may also play a role in olorofim susceptibility. A translation factor knockouts library screen revealed that deletion of HapB, AreA, DevR results in reduced susceptibility compared to WT isolates while deletion of transcription factor AcdX results in hypersensitivity [56]. However, similar *in vitro* resistance induction experiments were performed for triazole resistance in *A. fumigatus*. The mutations found in these *in vitro* experiments, like the amino acid substitutions at locus G54 and locus M220 in the *Cyp51A* gene can also be found in isolates retrieved from patients with CPA who are treated for long periods with triazoles, indicating that such *in vitro* experiments may predict the resistance mechanisms that can be found through clinical use [57,58].

As development of antifungal resistance is often associated with attenuated virulence [47], we investigated whether amino acid substitutions in *pyrE* at locus G119 mutations were associated with a fitness cost in *A. fumigatus*. Analysis of *A. fumigatus* with disrupted *chsC* and *chsG* which encode Class III chitin synthases, showed a reduced colony radial growth rate compared to the wildtype strain. Subsequent assessment of pathogenicity in neutropenic mice showed a reduction in mortality in the mice inoculated with a *chsC* and *chsG* disrupted strain compared to the wildtype isolates [59]. Similar correlations between growth rate and virulence were observed when the growth rate of *A. fumigatus* was assessed in 96-wells plates using the optical density as indicator for growth rate [45]. To understand whether *PyrE* amino-acid substitutions influence fitness of *A. fumigatus* which may be extrapolated to *in vivo* pathogenicity, we analyzed the radial growth rate of five isolates with *PyrE* substitutions. These experiments showed a small but significant reduction in growth rate for strains with a G119V substitution (strain AZN8196_OLR1 and Af293_OLR9), while strains with a G119C substitution did not exhibit a reduction in growth rate. These *in vitro* findings were confirmed in the *in vivo* pathogenicity model whereas no significant difference in survival was observed for isolates with a G119C amino acid substitution (isolates AZN8196_OLR2 and Af293_OLR7). These results indicate that the amino acid substitution affects the binding of olorofim to DHODH but may not affect the function of DHODH itself and the effect on DHODH function is dependent on the underlying amino acid substitution. However, a limitation of this observation is the low number of isolates that were tested. Furthermore, compensatory

evolution has been shown to occur in triazole-resistant *A. fumigatus* isolates when cultured in azole-free conditions, indicating that a potential fitness cost can be overcome [60]. However, population dynamics such as competition with other (wildtype) genotypes and selection pressure will ultimately determine which genotype will become dominant.

Olorofim represents an important new treatment option for patients with difficult to treat invasive fungal infections, including triazole-resistant *A. fumigatus* infection. Our study provides insights into one mechanism and potential dynamics of olorofim resistance, which will help to prevent and manage resistance selection in various patient groups. Such insights are critical to antifungal stewardship and to safeguard its prolonged use in clinical practice.

Acknowledgements

We thank Norman van Rhijn for discussion about the CRISPR-Cas9 design.

Disclosure statement

J.B reports grants from F2G Ltd and Gilead Sciences. J.O, D.L and M.B. are employees and shareholders of F2G Ltd. P.E. reports grants from Mundipharma, F2G Ltd, Pfizer, Gilead Sciences, and Cidara and nonfinancial support from IMMY for work outside the submitted study.

Funding

The study was supported by funding from F2G Ltd.

Data availability statement

All data can be requested by the corresponding author upon request.

References

- [1] Bongomin F, Gago S, Oladele RO, et al. Global and multi-national prevalence of fungal diseases-estimate precision. *J Fungi*. 2017 Oct 18;3(4):E57.
- [2] van de Veerdonk FL, Kolwijck E, Lestrade PP, et al. Influenza-associated aspergillosis in critically ill patients. *Am J Respir Crit Care Med*. 2017 Aug 15;196(4):524–527.
- [3] Schauwvlieghe A, Rijnders BJA, Philips N, et al. Invasive aspergillosis in patients admitted to the intensive care unit with severe influenza: a retrospective cohort study. *Lancet Respir Med*. 2018 Oct;6(10):782–792.
- [4] White PL, Dhillon R, Cordey A, et al. A national strategy to diagnose COVID-19 associated invasive fungal disease in the ICU. *Clin Infect Dis*. 2020 Aug 29;73(7):e1634–e1644.
- [5] Lamoth F, Glampedakis E, Boillat-Blanco N, et al. Incidence of invasive pulmonary aspergillosis among critically ill COVID-19 patients. *Clin Microbiol Infect*. 2020 Jul 10;26(12):1706–1708.

- [6] Dupont D, Menotti J, Turc J, et al. Pulmonary aspergillosis in critically ill patients with Coronavirus disease 2019 (COVID-19). *Med Mycol*. 2020 Sep 10;59(1):110–114.
- [7] Patterson TF, Thompson GR, 3rd, Denning DW, et al. Practice guidelines for the diagnosis and management of aspergillosis: 2016 update by the infectious diseases society of America. *Clin Infect Dis*. 2016 Aug 15;63(4):e1–e60.
- [8] Ullmann AJ, Aguado JM, Arikan-Akdagli S, et al. Diagnosis and management of Aspergillus diseases: executive summary of the 2017 ESCMID-ECMM-ERS guideline. *Clin Microbiol Infect*. 2018 May;24(Suppl 1):e1–e38.
- [9] Aruanno M, Glampedakis E, Lamoth F. Echinocandins for the treatment of invasive aspergillosis: from laboratory to bedside. *Antimicrob Agents Chemother*. 2019 Aug;63(8):e00399–19.
- [10] Adler-Moore J, Lewis RE, Brüggemann RJM, et al. Preclinical safety, tolerability, pharmacokinetics, pharmacodynamics, and antifungal activity of liposomal amphotericin B. *Clin Infect Dis*. 2019 May 2;68(Suppl 4):S244–s259.
- [11] Verweij PE, Chowdhary A, Melchers WJ, et al. Azole resistance in *Aspergillus fumigatus*: can we retain the clinical use of mold-active antifungal azoles? *Clin Infect Dis*. 2016 Feb 01;62(3):362–368.
- [12] Buil JB, Snelders E, Denardi LB, et al. Trends in azole resistance in *Aspergillus fumigatus*, the Netherlands, 1994–2016. *Emerg Infect Dis*. 2019 Jan;25(1):176–178.
- [13] Lestrade PPA, Buil JB, van der Beek MT, et al. Paradoxal trends in azole-resistant *Aspergillus fumigatus* in a national multicenter surveillance program, the Netherlands, 2013–2018. *Emerg Infect Dis*. 2020 Jul;26(7):1447–1455.
- [14] Lestrade PP, Bentvelsen RG, Schauwvlieghe A, et al. Voriconazole resistance and mortality in invasive aspergillosis: a multicenter retrospective Cohort study. *Clin Infect Dis*. 2019 Apr 24;68(9):1463–1471.
- [15] Verweij PE, Snelders E, Kema GH, et al. Azole resistance in *Aspergillus fumigatus*: a side-effect of environmental fungicide use? *Lancet Infect Dis*. 2009 Dec;9(12):789–795.
- [16] Jones ME. Pyrimidine nucleotide biosynthesis in animals: genes, enzymes, and regulation of UMP biosynthesis. *Annu Rev Biochem*. 1980;49:253–279.
- [17] Oliver JD, Sibley GE, Beckmann N, et al. F901318 represents a novel class of antifungal drug that inhibits dihydroorotate dehydrogenase. *Proc Natl Acad Sci USA*. 2016 Oct 25;113(45):12809–12814.
- [18] Astvad KMT, Jørgensen KM, Hare RK, et al. Olorofim susceptibility testing of 1423 Danish mould isolates 2018–2019 confirms uniform and broad-spectrum activity. *Antimicrob Agents Chemother*. 2020 Oct 5;65(1):e01527–20.
- [19] du Pré S, Beckmann N, Almeida MC, et al. Effect of the novel antifungal drug F901318 (olorofim) on growth and viability of *Aspergillus fumigatus*. *Antimicrob Agents Chemother*. 2018;62(8):e00231–18.
- [20] Jørgensen KM, Astvad KMT, Hare RK, et al. EUCAST determination of olorofim (F901318) susceptibility of mold species, method validation, and MICs. *Antimicrob Agents Chemother*. 2018;62(8):e00487–18.
- [21] Seyedmousavi S, Chang YC, Law D, et al. Efficacy of olorofim (F901318) against *Aspergillus fumigatus*, *A. nidulans*, and *A. tanneri* in murine models of profound neutropenia and chronic granulomatous disease. *Antimicrob Agents Chemother*. 2019;63(6):e00129–19.
- [22] Buil JB, Rijs A, Meis JF, et al. In vitro activity of the novel antifungal compound F901318 against difficult-to-treat *Aspergillus* isolates. *J Antimicrob Chemother*. 2017 Sep 1;72(9):2548–2552.
- [23] Rivero-Menendez O, Cuenca-Estrella M, Alastruey-Izquierdo A. In vitro activity of olorofim (F901318) against clinical isolates of cryptic species of *Aspergillus* by EUCAST and CLSI methodologies. *J Antimicrob Chemother*. 2019;74(6):1586–1590.
- [24] Negri CE, Johnson A, McEntee L, et al. Pharmacodynamics of the novel antifungal agent F901318 for Acute Sinopulmonary Aspergillosis caused by *Aspergillus flavus*. *J Infect Dis*. 2018;217(7):1118–1127.
- [25] Hope WW, McEntee L, Livermore J, et al. Pharmacodynamics of the orotomides against *Aspergillus fumigatus*: new opportunities for treatment of multidrug-resistant fungal disease. *mBio*. 2017;8(4):e01157–17.
- [26] Kirchhoff L, Dittmer S, Buer J, et al. In vitro activity of olorofim (F901318) against fungi of the genus, *Scedosporium* and *Rasamsonia* as well as against *Lomentospora prolificans*, *Exophiala dermatitidis* and azole-resistant *Aspergillus fumigatus*. *Int J Antimicrob Agents*. 2020 Sep;56(3):106105.
- [27] Kirchhoff L, Dittmer S, Weisner AK, et al. Antibiofilm activity of antifungal drugs, including the novel drug olorofim, against *Lomentospora prolificans*. *J Antimicrob Chemother*. 2020 Aug 1;75(8):2133–2140.
- [28] Rivero-Menendez O, Cuenca-Estrella M, Alastruey-Izquierdo A. In vitro activity of olorofim against clinical isolates of *Scedosporium* species and *Lomentospora prolificans* using EUCAST and CLSI methodologies. *J Antimicrob Chemother*. 2020 Aug 28;75(12):3582–3585.
- [29] Wiederhold NP, Law D, Birch M. Dihydroorotate dehydrogenase inhibitor F901318 has potent in vitro activity against *Scedosporium* species and *Lomentospora prolificans*. *J Antimicrob Chemother*. 2017 Mar 15;72(7):1977–1980.
- [30] Biswas C, Law D, Birch M, et al. In vitro activity of the novel antifungal compound F901318 against Australian *Scedosporium* and *Lomentospora* fungi. *Med Mycol*. 2018;56(8):1050–1054.
- [31] Wiederhold NP, Najvar LK, Jaramillo R, et al. The orotomide olorofim is efficacious in an experimental model of central nervous system coccidioidomycosis. *Antimicrob Agents Chemother*. 2018;62(9):e00999–18.
- [32] Lim W, Eadie K, Konings M, et al. *Madurella mycetomatis*, the main causative agent of eumycetoma, is highly susceptible to olorofim. *J Antimicrob Chemother*. 2020 Apr 1;75(4):936–941.
- [33] Wiederhold NP. Review of the novel investigational antifungal olorofim. *J Fungi*. 2020 Jul 30;6(3):122.
- [34] Singh A, Singh P, Meis JF, et al. In vitro activity of the novel antifungal olorofim against dermatophytes and opportunistic moulds including *Penicillium* and *Talaromyces* species. *J Antimicrob Chemother*. 2021 Apr 13;76(5):1229–1233.
- [35] Badali H, Cañete-Gibas C, Patterson H, et al. In vitro activity of olorofim against clinical isolates of the *Fusarium oxysporum* and *Fusarium solani* species complexes. *Mycoses*. 2021 Jul;64(7):748–752.

- [36] Lackner M, Birch M, Naschberger V, et al. Dihydroorotate dehydrogenase inhibitor olorofim exhibits promising activity against all clinically relevant species within *Aspergillus* section Terrei. *J Antimicrob Chemother.* **2018**;73(11):3068–3073.
- [37] Espinel-Ingroff A, Dawson K, Pfaller M, et al. Comparative and collaborative evaluation of standardization of antifungal susceptibility testing for filamentous fungi. *Antimicrob Agents Chemother.* **1995**;39(2):314–319.
- [38] Seyedmousavi S, Bruggemann RJ, Meis JF, et al. Pharmacodynamics of isavuconazole in an *Aspergillus fumigatus* mouse infection model. *Antimicrob Agents Chemother.* **2015 May**;59(5):2855–2866.
- [39] Buil JB, Bruggemann RJM, Wasmann RE, et al. Isavuconazole susceptibility of clinical *Aspergillus fumigatus* isolates and feasibility of isavuconazole dose escalation to treat isolates with elevated MICs. *J Antimicrob Chemother.* **2018 Jan 1**;73(1):134–142.
- [40] Buil JB, van der Lee HAL, Rijs A, et al. Single-center evaluation of an agar-based screening for azole resistance in *Aspergillus fumigatus* by using VIPcheck. *Antimicrob Agents Chemother.* **2017 Dec**;61(12):e01250–17.
- [41] Bertuzzi M, van Rhijn N, Krappmann S, et al. On the lineage of *Aspergillus fumigatus* isolates in common laboratory use. *Med Mycol.* **2020**;59(1):7–13.
- [42] van Rhijn N, Furukawa T, Zhao C, et al. Development of a marker-free mutagenesis system using CRISPR-Cas9 in the pathogenic mould *Aspergillus fumigatus*. *Fungal Genet Biol.* **2020**;145:103479.
- [43] Peng D, Tarleton R. EuPaGDT: a web tool tailored to design CRISPR guide RNAs for eukaryotic pathogens. *Microb Genom.* **2015 Oct**;1(4):e000033.
- [44] Seyedmousavi S, Mouton JW, Melchers WJG, et al. In vivo efficacy of liposomal amphotericin B against wild-type and azole-resistant *Aspergillus fumigatus* isolates in two different immunosuppression models of invasive aspergillosis. *Antimicrob Agents Chemother.* **2017 Jun**;61(6):e02479–16.
- [45] Paisley D, Robson GD, Denning DW. Correlation between in vitro growth rate and in vivo virulence in *Aspergillus fumigatus*. *Med Mycol.* **2005 Aug**;43(5):397–401.
- [46] Samson RA, Visagie CM, Houbraeken J, et al. Phylogeny, identification and nomenclature of the genus *aspergillus*. *Stud Mycol.* **2014 Jun**;78:141–173.
- [47] Arendrup MC, Mavridou E, Mortensen KL, et al. Development of azole resistance in *Aspergillus fumigatus* during azole therapy associated with change in virulence. *PLoS One.* **2010**;5(4):e10080.
- [48] Howard SJ, Cerar D, Anderson MJ, et al. Frequency and evolution of Azole resistance in *Aspergillus fumigatus* associated with treatment failure. *Emerg Infect Dis.* **2009 Jul**;15(7):1068–1076.
- [49] Ballard E, Melchers WJG, Zoll J, et al. In-host microevolution of *Aspergillus fumigatus*: a phenotypic and genotypic analysis. *Fungal Genet Biol.* **2018 Apr**;113:1–13.
- [50] Bongomin F, Harris C, Hayes G, et al. Twelve-month clinical outcomes of 206 patients with chronic pulmonary aspergillosis. *PLoS One.* **2018**;13(4):e0193732.
- [51] Dudakova A, Spiess B, Tangwattanachuleeporn M, et al. Molecular tools for the detection and deduction of azole antifungal drug resistance phenotypes in *Aspergillus* species. *Clin Microbiol Rev.* **2017 Oct**;30(4):1065–1091.
- [52] D’Enfert C, Diaquin M, Delit A, et al. Attenuated virulence of uridine-uracil auxotrophs of *Aspergillus fumigatus*. *Infect Immun.* **1996 Oct**;64(10):4401–4405.
- [53] Retallack DM, Heinecke EL, Gibbons R, et al. The URA5 gene is necessary for histoplasma capsulatum growth during infection of mouse and human cells. *Infect Immun.* **1999**;67(2):624–629.
- [54] Noble SM, Johnson AD. Strains and strategies for large-scale gene deletion studies of the diploid human fungal pathogen *Candida albicans*. *Eukaryot Cell.* **2005 Feb**;4(2):298–309.
- [55] de Gontijo FA, Pascon RC, Fernandes L, et al. The role of the de novo pyrimidine biosynthetic pathway in *Cryptococcus neoformans* high temperature growth and virulence. *Fungal Genet Biol.* **2014 Sep**;70:12–23.
- [56] van Rhijn N, Hemmings S, Valero C, et al. Olorofim and the azoles are antagonistic in *A. fumigatus* and functional genomic screens reveal mechanisms of cross resistance. *bioRxiv.* **2021**:2021.11.18.469075.
- [57] Escribano P, Recio S, Peláez T, et al. In vitro acquisition of secondary azole resistance in *Aspergillus fumigatus* isolates after prolonged exposure to itraconazole: presence of heteroresistant populations. *Antimicrob Agents Chemother.* **2012 Jan**;56(1):174–178.
- [58] da Silva Ferreira ME, Capellaro JL, dos Reis Marques E, et al. In vitro evolution of itraconazole resistance in *Aspergillus fumigatus* involves multiple mechanisms of resistance. *Antimicrob Agents Chemother.* **2004**;48(11):4405–4413.
- [59] Mellado E, Aufauvre-Brown A, Gow NA, et al. The *Aspergillus fumigatus* *chsC* and *chsG* genes encode class III chitin synthases with different functions. *Mol Microbiol.* **1996 May**;20(3):667–679.
- [60] Verweij PE, Zhang J, Debets AJM, et al. In-host adaptation and acquired triazole resistance in *Aspergillus fumigatus*: a dilemma for clinical management. *Lancet Infect Dis.* **2016 Nov**;16(11):e251–e260.